# Rhinoplasty Pre-Surgery Models by Using Low-Dose Computed Tomography, Magnetic Resonance Imaging, and 3D Printing

Dario Baldi[1] , Luca Basso[1] , Gisella Nele[1], Giovanni Federico[1],
Giuseppe Walter Antonucci[2], Marco Salvatore[1], and Carlo Cavaliere[1]

## Abstract
Rhinoplasty and surgical reconstruction of cartilaginous structures still remain a great challenge today. This study aims to identify an imaging strategy in order to merge the information from CT scans and magnetic resonance imaging (MRI) acquisitions and build a 3D printed model true to the patient's anatomy, for better surgical planning. Using MRI, information can be obtained about the cartilage structures of which the nose is composed. Ten rhinoplasty candidate patients underwent both a low-dose protocol CT scan and a specific MRI for characterization of nasal structures. Bone and soft tissue segmentations were performed in CT, while cartilage segmentations were extrapolated from MRI and validated by both an expert radiologist and surgeon. Subsequently, a 3D model was produced in materials and colors reproducing the density of the three main structures (bone, soft tissue, and cartilage), useful for pre-surgical evaluation. This study has highlighted that the optimization of a CT and MR dedicated protocol has allowed to reduce the CT radiation dose up to 60% compared to standard acquisitions with the same machine, and MR acquisition time of about 20%. Patient-tailored 3D models and pre-surgical planning have reduced the mean operative time by 20 minutes.

## Keywords
LDCT, MRI, 3D printing, rhinoplasty

## Introduction

Rhinoplasty is a plastic surgery procedure aimed at improving the nose's appearance and function. According to 2019s statistics provided by the American Society of Plastic Surgeons, 207,000 rhinoplasties have been performed in the United States. Different rhinoplasty surgery procedures have been described in the literature, namely, the open and the close approaches.[1] The most frequent approach is the open one, which produces optimal visualizations of the different anatomical nose tissues and components.[2] Visualizing such anatomical structures appropriately may improve surgical outcomes.[3] Indeed, most limiting conditions to rhinoplasty originate in the low diagnostic imaging capacity to characterize this region in the pre-surgical phase.[4] More frequently, the nose's structures are studied using computed tomography.[5] Such technology allows the high spatial resolution analysis of most parts of the nose, especially the bone components. However, CT has a non-negligible biological risk related to the high amount of ionizing radiation emitted by the scanner. Also, CT fails to characterize the nose's cartilages, which are of primary importance in defining the shape of the nose. Indeed, these structures vary from individual to individual, constituting the main surgical target when surgeons remodel nasal profiles. Considerable efforts have been made to develop workarounds for the abovementioned shortcomings. Indeed, third-generation Dual-Source CT scanners (DSCT) and the most recent dose-reduction CT acquisition

[1]IRCCS SDN, Naples, Italy
[2]U.O.S.V.D. Radiologia Territoriale-ASL BT, Trani, Italy

**Corresponding Author:**
Luca Basso, IRCCS SDN, via E.Gianturco 113, Naples 80143, Italy.
Email: luca.basso@synlab.it

protocols allow obtaining tissue characterizations whose results are comparable with standard CT scanners but with a significant reduction of ionizing radiation. DSCT for studying both the facial massif and the nose is based on the combined use of two X-ray tubes coupled with a tin filter. The tin filter absorbs low-energy photons, which are less important in high-contrast settings (e.g., maxillo-facial imaging), thus reducing patients' radiation exposure. In this field, using a tube voltage of 100 kV, a reduced tube current, and iterative reconstructions produce new interesting perspectives in low-dose imaging.[6] Paralleling CT improvements, magnetic resonance imaging (MRI) has also gained diagnostic accuracy in this field, thanks to the development of more resolute sequences and dedicated protocols. Recently developed MRI sequences permit a better study of nasal cartilage structures, which results in an improved characterization of the median septal cartilage, the two lateral cartilages, and the two major alar cartilages. Visscher et al. compared various types of MRI sequences, in order to identify the one that best characterizes the cartilage structures of the nose. Cartilage-specific sequences were compared: Constructive Interference in Steady State (CISS), Fast Spin Echo (FSE), Multiple Echo Recombined Gradient Echo, and Spoiled Gradient Echo (Spoiled GE) with and without fat suppression. The result highlights that the Spoiled GE sequence without fat suppression with a spatial resolution of 0.9 mm has better sensitivity and specificity for visualization of cartilages, especially for the alar one.[7] Moreover, the most interesting advances to support the study of nasal structures come from personalized medicine and concern the improvements achievable by combining imaging techniques with biomedical engineering. Customized, imaging-derived, 3D printed models may provide a helpful visual reference of the scanned anatomical structures, hence permitting to anticipate surgery planning and reduce surgical times.[8,9] The aim of this paper is to highlight the clinical value of 3D printed models in helping to align patient and surgeon goals in the preoperative and consultative setting. This combined radiological-bioengineristic-surgical approach may strengthen the value of custom surgical templates for use as operative blueprints to facilitate intraoperative decision-making in rhinoplasty. For this reason, we have developed an affordable and reproducible protocol, for rapid in-house 3D printed rhinoplasty models for surgical planning, starting from low-dose CT acquisition protocol and high-resolution MRI dedicated protocol.

## Material and Methods

### Patient Population

This retrospective study was approved by the Institutional Review Board, and all patients signed a dedicated informed consent. Ten consecutive adult patients who underwent maxillo-facial DECT and MRI, examined at IRCCS SDN, Naples (IT), from September 2020 to April 2021, were included. The selected patients were all candidates for rhinoplasty. Inclusion criteria were the following: patient's age >18 years, no pregnancy status, no further pathology of the maxillo-facial area, and no prosthesis and/or metal wire inside the body not compatible with high-field magnetic resonance.

### Acquisition Protocols

The CT scans were performed using a third-generation DSCT scanner (SOMATOM Force, Siemens Health care, Germany). Left tube voltage was fixed to 100 kV with a 0.6 mm tin filter, and tube current was set to 130 mAs. Automatic tube current modulation (CARE Dose 4D, Siemens) and automated tube potential control (CARE kV, Siemens) were turned off. Patients were scanned in a supine position with the head slightly reclined to take an around parallel alignment of the upper jaw to the gantry to minimize artifacts due to any dental prosthesis. The scan range extended from the frontal sinus down to the maxilla. Axial 1 mm images were reconstructed using both an iterative bone (Hr64) and soft tissue (Br40) reconstruction filter (ADMIRE, Siemens, IR resistance level 3 [bone] and 4 [soft tissue], respectively). The MRI scans were acquired with a 3T Achieva dStream scanner (Philips Health care, Best, Netherlands), and a 16-channel head-neck coil. In addition, foam pads were used to minimize any patient movement. A 3D axial Spoiled GE without fat saturation sequence was acquired with the following parameters: TR 5.9 ms; TE 2.51 ms; Flip Angle 12; Average 2 and Slice Thickness 1 mm was used to allow a better characterization of the nasal cartilages. Both CT and MRI acquisitions have been following co-registered in Syngo. via platform (Syngo.via Workstation; Siemens Health care), for mutual imaging segmentation.

### Computed Tomography Scan Radiation Dosimetry

The value of the effective radiation dose (ED) was based on the volume computed tomography dose index (CTDI) and dose length product (DLP), which were recorded from the "dose report," which is automatically stored in the DICOM.

A conversion factor for the head region (0.0019 mSv x mGy-1 x cm-1; reference to the 16 cm CTDI phantom) was used for calculating the ED.

The effective dose results as follows: ED = DLP x 0.0019 mSv x mGy-1.

An additional conversion factor of 2.5 was applied to compensate for the different reference phantoms. All CTDIvol values following are referring to the 16-cm phantom.

The optimized protocol allowed a CTDIvol of about 18.33 mGy [range 11.66-21.77 mGy]. The median DLP was 382 mGy*cm [range 268–460 mGy*cm]. The resulting median effective radiation dose was 0.725 mSv [range 0.51–0.87 mSv].
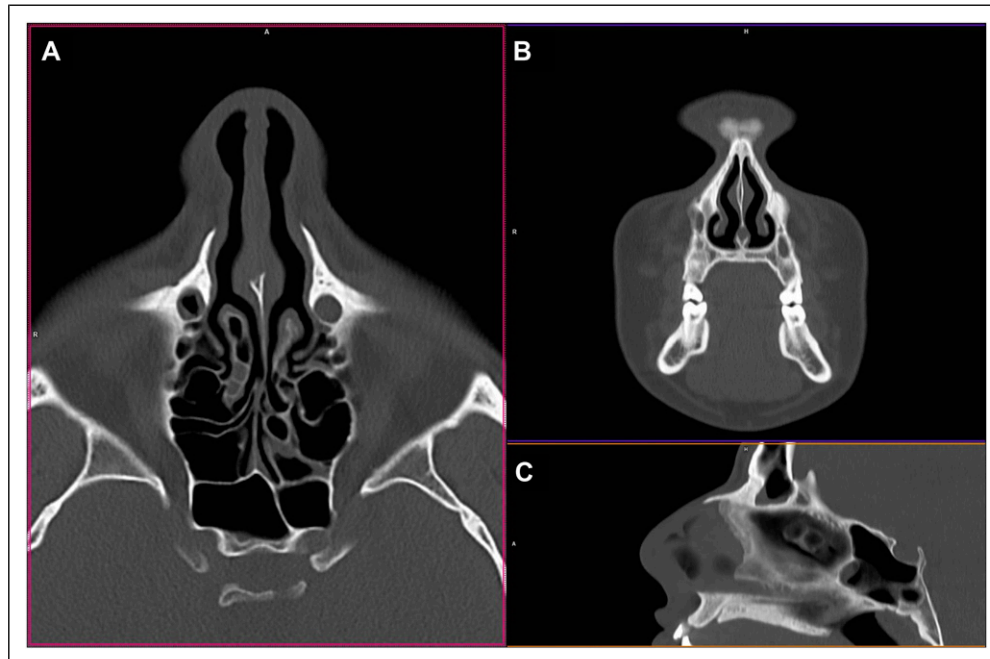
**Figure 1.** Axial (A), coronal (B) and sagittal (C) reconstruction from low-dose maxillo-facial CT scan, using an iterative bone reconstruction filter.

## Computed Tomography Image Segmentation

The CT digital imaging and communications in medicine (DICOM) can be segmented using manual, semi-automatic, and automatic techniques.[11,12] The DICOM files were imported into the Mimics 21 medical image segmentation program (Materialise NV, Leuven).

Using this software, it is possible to perform a semi-automatic segmentation of the main tissues (i.e., bones, fat, etc.) that make up the anatomy of the nose. This is possible by associating the density of each tissue, expressed in grayscale and detected by CT, with a different color. Subsequently, a manual correction of any burrs was performed by an experienced radiologist and then confirmed by the surgeon. At the end of the segmentation phase, a digital 3D model faithful to the original anatomy, and life-sized, was built.[13]

Two different types of structures have been defined and segmented, "bone" and "soft tissue" (skin, mucosa, and cartilages), to which different printing materials were associated, which allowed for as much anatomical reproduction as possible (Figure 1).

## Magnetic Resonance Imaging Segmentation

The DICOM of the MRI sequence was imported into the ITK-SNAP software.[14] A user-guided 3D segmentation of cartilage anatomical structures was performed. In particular, the segmentation of the alar cartilage, the lateral cartilage of the nose, and the cartilage of the septum were carried out, which

are better represented in the MRI scan, compared to CT acquisition.

## Mutual Imaging Information and Model Building

The 3D digital models (STL files) obtained in the segmentation step by CT and MRI were fused and further processed using the 3-Matic software package (Materialise, Belgium), which allows direct STL manipulation, error control, the closing of small holes, surface smoothing, and part thickness analysis. In a preliminary phase, MRI segmented volumes were superimposed to CT ones, in order to differentiate cartilaginous structures highlighted by MRI within the soft tissue volume extracted by CT (Figure 2). Following, data conditioning, including smoothing rough surfaces, removing items that could lead to printing errors, and performing procedures such as notching parts to achieve the final model of the nose, was performed (Figure 3).[13]

## Model Printing Preparation

The STL file has been exported to the open-source CURA 4.8 software (Ultimaker, Netherlands) for slicing. Subsequently, the STL file is converted into layers (generating contour data), produces the toolpaths on XYZ axes to fill them, and determines the filament's quantity to be used in the manufacturing of the product. The toolpath is defined by G-code files generated for each layer of the product, and these codes provide the instruction for the X, Y, and Z
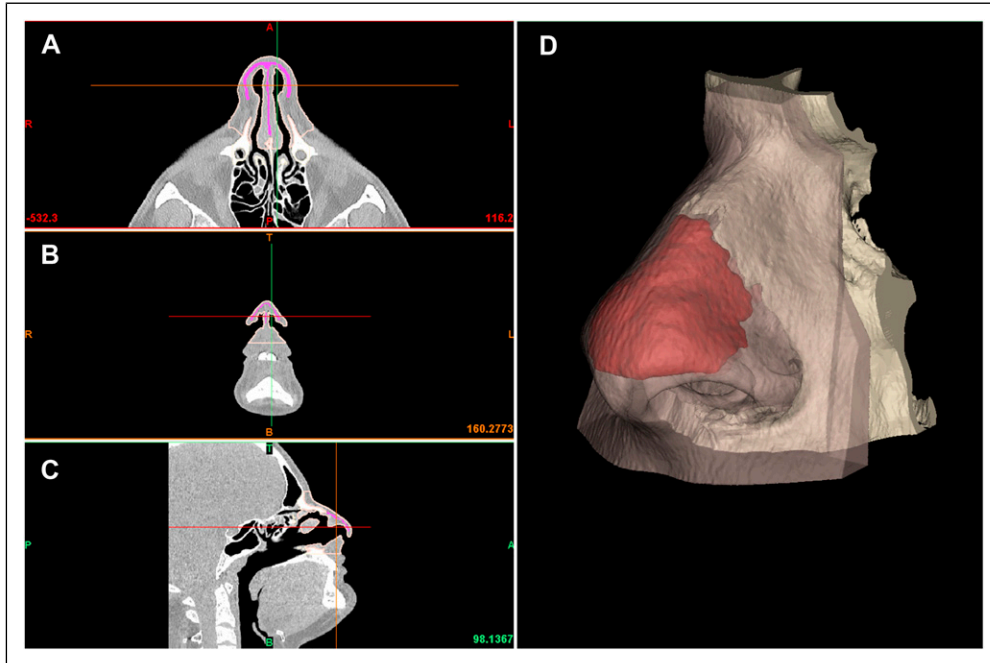
**Figure 2.** Segmentation phase, on the left the multiplanar reconstructions on the axial (A), coronal (B) and sagittal planes (C), in pink the mask imported post-segmentation from MRI. On the right (D), the 3D models of the bone tissue in white, the cartilage structures in red (from MRI/CT coregistration), and the soft tissues of the nasal pyramid in pink (in transparency).
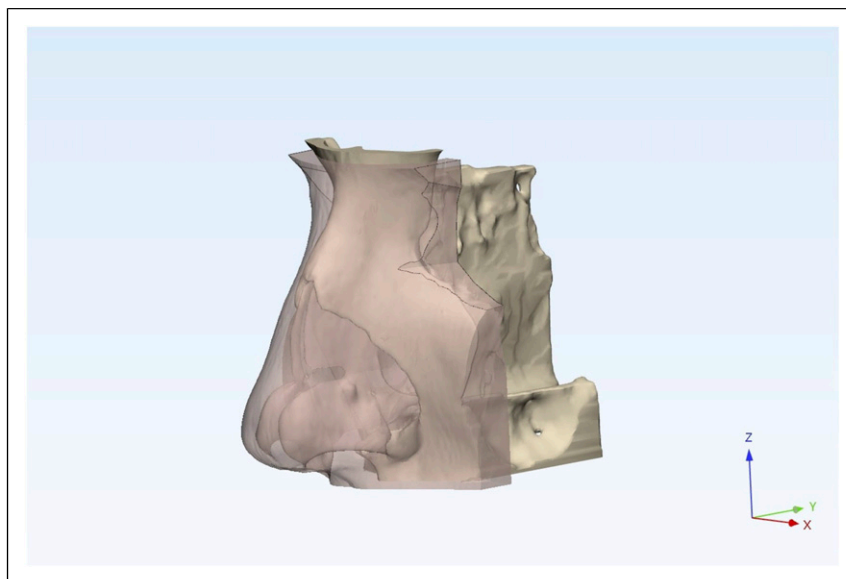


**Figure 3.** Print model preparation phase, performed on 3D-matic software; 3D models of bone and soft tissue are shown in the figure, after removal of segmentation errors.

motion of the tool to generate the required layers. The CURA software can perform most of the preparatory processes for STL files for fused deposition modeling (FDM) technology printing; these include machine platform, heating of the printing plate to promote adhesion, adjusting orientation, repairing parts, generating necessary supports, and positioning the model. The models used in this study are simple and do not require support structures (Figure 4).
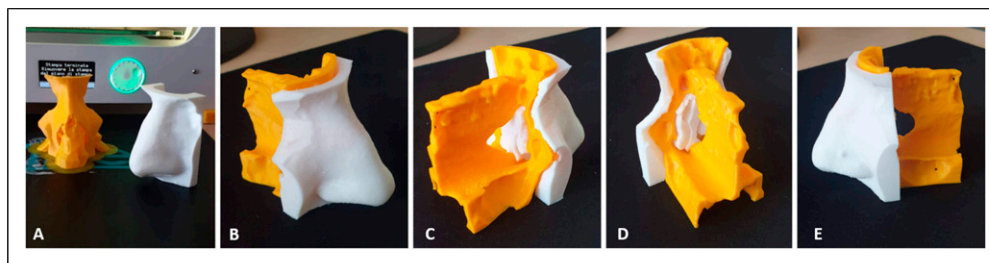
## Printing

This study's filament materials were polylactic acid (PLA) and thermoplastic polyurethane (TPU). These filaments are
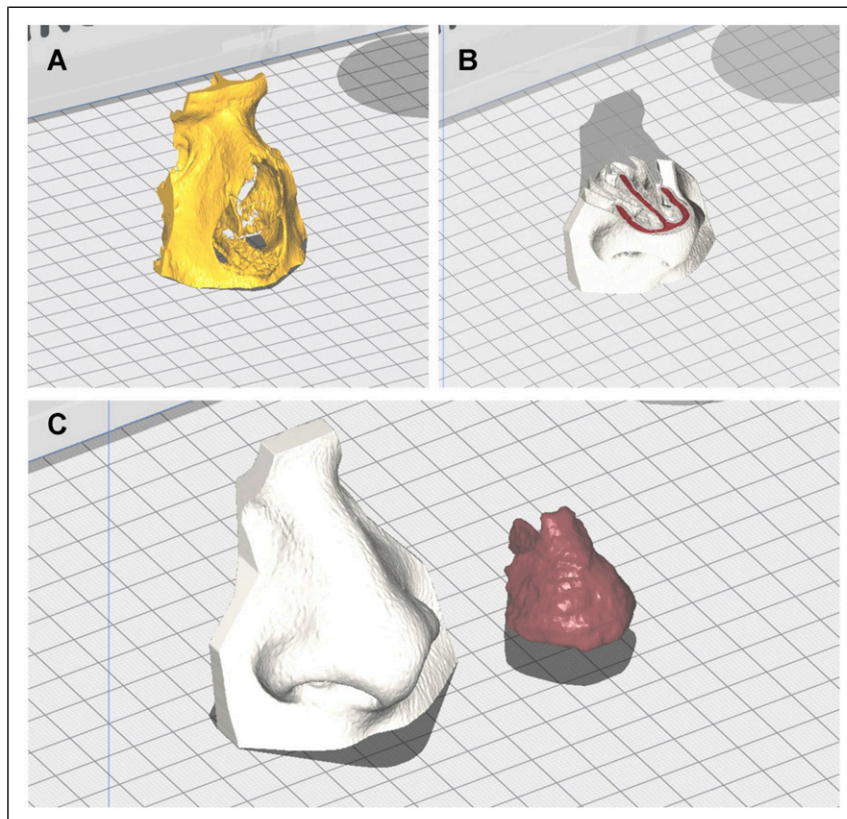
**Figure 4.** Slicing phase with Cura software. Image A shows the bone tissue model (in yellow), subsequently printed with PLA; in inset B, the soft tissue (in white) and cartilage (in red) to show the anatomically correct position of the two models; image C show the two adjacent soft tissue (in white) and cartilage (in red) models, printed in TPU.



**Figure 5.** The image shows custom 3D models of the bone component (in white) and soft tissue (in yellow), also embedded within each other.

preferred by most domestic 3D printers across the world since it is easy to print; they have an extruding temperature ranging between 180°C and 210°C. The material is bioplastic and non-toxic and therefore has extensive biomedical applications.[14] The 3D printing of the samples was undertaken using the 3D printer, Ultimaker 3EXT.

In particular, we used PLA to create bone components, and two different colors of TPU to distinguish cartilage (red color) from other soft tissues (white color), like skin and mucosa. The realization of the model consumed about 26 g of PLA for the bone structures and 35 g of TPU to reproduce

soft tissues for about 3.5 euros of material consumed (printing time: 4.5 h) (Figure 5).[15]

## Discussion

3D imaging, from CT and MRI scans, has become a popular and widespread imaging modality in aesthetic surgery. In rhinoplasty, 3D imaging with the simulation of expected surgical results has improved patient communication in surgical planning,[16] and may lead to an increase in postoperative patient satisfaction.[17] Leveraging 3D imaging to create patient-

specific 3D models has also been demonstrated to optimize intraoperative execution in a variety of surgical fields,[18] although its application for nasal reconstruction surgery has been poorly investigated.

Rhinoplasty is a complicated procedure known to require meticulous planning and precise execution to obtain optimal results. Rhinoplasty also has an important place in aesthetic surgery. In fact, potential psychological determinants underlying the choice of such a surgical procedure might be traced in the link between rhinoplasty, psychology, and social environment.[19] Also, the nose has a central role in self and other's face perception as it constitutes, alongside mouth and eyes, a major visual-attentional target for individuals involved in face exploration.[20]

Rhinoplasty is undoubtedly one of the most challenging surgeries to master within the specialty and makes matters more complicated; it is also one of the least commonly encountered training procedures. Nowadays, rhinoplasty can be performed as structured rhinoplasty or as preservation rhinoplasty. In structured rhinoplasty, the dorsal hump is removed. An open roof is created and closed with basal fractures while the cartilaginous dorsum can be reconstructed with stitches, spreader flaps, or grafts.

In preservation rhinoplasty, the dorsum is preserved and modified to remove the dorsal hump. Not every patient has the indication for preservation rhinoplasty and when a preservation rhinoplasty is performed, an accurate preoperative evaluation must be done on a 3D CT scan to avoid dangerous complications. Moreover, during preservation rhinoplasty, surgeons must know where to perform radix osteotomy and where the E point is (the point between the perpendicular plate of the ethmoid and the quadrangular cartilage) to be safe during these kinds of maneuvers.[21]

Advanced volumetric CT/MR imaging is mandatory to assess patient anatomy and should be used to choose between structured or preservation rhinoplasty approaches, to choose among the different preservation techniques (e.g., high strip preservation, low strip preservation, or cartilaginous preservation), and to measure anatomy landmarks. In all these phases, 3D modeling can help to better manage the patient, allowing to simulate each branch of the possible decision tree and to actively recognize anatomical landmarks as transverse radix osteotomy point (TROP) to avoid surgical complications.[4] For instance, it is important to identify any part of the perpendicular plate of the ethmoid before surgery, to avoid dangerous maneuvers and fracture to the cribriform plate, with consequent cerebrospinal fluid leakage.

3D printing is becoming more popularized in the medical field due to technical planning, patient communication, and this challenging operation's performance.

Many studies have shown that 3D printed models provide excellent support to the world of medicine, in the dental, anatomical–pathological, and surgical fields, thanks to the possibility of planning the intervention first on a model that perfectly imitates the anatomy and pathology.

The added value of the tailored 3D modeling compared to the native 3D imaging techniques are represented by a better understanding of patients' anatomy (internal and external nasal anatomy); better compliance for the patients that can understand their own anatomy; the possibility to estimate and predict surgical maneuvers; the reduction of operating time and costs (as these kinds of surgeries are usually performed as private surgeries); and the reduction of postoperative complications such as CSF leakage, insufficient functional treatment, and poor aesthetic results due to unsuccessful maneuvers.

Contemplating how the different maneuvers will occur in the sequence is critical but knowing how each move will subsequently affect the procedure or the next few choices is essential to obtaining reproducible and good results. The model proposes several opportunities: it will allow surgeons to pre-operatively plan their cartilaginous changes and osteotomies and better visualize the underlying pathology; this will undoubtedly allow for improved planning and understanding of how the photographs correlate the structural anatomy.

One study has recently demonstrated that plastic surgery trainee confidence and hands-on experience in rhinoplasty are highly variable and often suboptimal.[22]

The acquisition of such skills is challenging, as plastic surgeons involved in teaching residents must balance providing trainees hands-on experience to become proficient in rhinoplasty techniques while ensuring the appropriate execution of such maneuvers to avoid unsatisfactory results.[23,24]

In our preliminary experience, the optimization of a CT and MR dedicated protocol has allowed to reduce the CT radiation dose up to 60% compared to standard acquisitions with the same machine, and MR acquisition time of about 20%. Patient-tailored 3D models and pre-surgical planning have reduced the mean operative time by 20 minutes. Also, no complications have been reported in preservation rhinoplasties performed with the described multidisciplinary approach. The model is patient-specific and can be used to visualize various nasal changes including tip alteration, dorsum reduction, and asymmetry correction, amongst others. This workflow incorporates evolving technology with 3D printing, while still acknowledging a surgeon's need to adapt intraoperatively based on his or her surgical experience and intuition. This surgical workflow we described fits into existing clinical workflows and may offer significant clinical benefits to patients and surgeons. It poses a modest financial expense and requires little or no additional technical expertise or training for the surgeon and moderate expertise/training for a radiological technician (for printing part).

## Declaration of Conflicting Interests

## ORCID iDs

Dario Baldi ⓘ https://orcid.org/0000-0001-7464-4499
Luca Basso ⓘ https://orcid.org/0000-0002-1774-0924
Carlo Cavaliere ⓘ https://orcid.org/0000-0002-3297-2213

## References

1. Daniel RK. *Rhinoplasty.* New York: Springer; 2002. doi:10.1007/978-1-4757-4262-6

2. Cafferty A, Becker DG. Open and closed rhinoplasty. *Clin Plas Surg.* 2016;43(1):17-27. doi:10.1016/j.cps.2015.09.002.

3. Sena Esteves S, Gonçalves Ferreira M, Carvalho Almeida J, Abrunhosa J. Almeida e Sousa C. Evaluation of aesthetic and functional outcomes in rhinoplasty surgery: a prospective study. *Brazilian J Otorhinolaryng.* 2017;83(5):552-557. doi:10.1016/j.bjorl.2016.06.010.

4. Sadri A, East C, Badia L, Saban Y. Dorsal preservation rhinoplasty: core beam computed tomography analysis of the nasal vault, septum, and skull base—its role in surgical planning. *Facial Plast Surg.* 2020;36(03):329-334. doi:10.1055/s-0040-1712538.

5. Jahandideh H, Maleki Delarestaghi M, Jan D, Sanaei A. Assessing the clinical value of performing CT scan before rhinoplasty surgery. *Intern J Otolaryng.* 2020;2020:1-7. doi:10.1155/2020/5929754.

6. Baldi D, Tramontano L, Alfano V, Punzo B, Cavaliere C, Salvatore M. Whole body low dose computed tomography using third-generation dual-source multidetector with spectral shaping: protocol optimization and literature review. *Dose-Response.* 2020;18(4):155932582097313. doi:10.1177/1559325820973131.

7. Visscher DO, van Eijnatten M, Liberton NPTJ, et al. MRI and additive manufacturing of nasal alar constructs for patient-specific reconstruction. *Sci Rep.* 2017;7(1):10021. doi:10.1038/s41598-017-10602-9.

8. Ballard DH, Mills P, Duszak R, Weisman JA, Rybicki FJ, Woodard PK. Medical 3D printing cost-savings in orthopedic and maxillofacial surgery: cost analysis of operating room time saved with 3D printed anatomic models and surgical guides. *Academic Radio.* 2020;27:1103-1113. doi:10.1016/j.acra.2019.08.011.

9. Vitali J, Cheng M, Wagels M. Utility and cost–effectiveness of 3D-printed materials for clinical use. *J 3D Print Med.* 2019;3(4):209-218. doi:10.2217/3dp-2019-0015.

10. ICRP publication 103. Protection Radiological. The 2007 Recommendations of the International Commission on Radiological Protection. *Ann ICRP 37.2.4* 2007;37(2-4):1-332. doi:10.1016/j.icrp.2007.10.003. In press.

11. Wardman K, Prestwich RJ, Gooding MJ, Speight RJ. The feasibility of atlas-based automatic segmentation of MRI for H&N radiotherapy planning. *J Appl Clin Med Phys.* 2016;17(4):146-154. doi:10.1120/jacmp.v17i4.6051.

12. Cuocolo R, Comelli A, Stefano A, et al. Deep learning whole-gland and zonal prostate segmentation on a public MRI dataset. *J Magn Reson Imag.* 2021;54(2):452-459. doi:10.1002/jmri.27585.

13. Feng Z-H, Li X-B, Phan K, et al. Design of a 3D navigation template to guide the screw trajectory in spine: a step-by-step approach using mimics and 3-Matic software. *J Spine Surg.* 2018;4(3):645-653. doi:10.21037/jss.2018.08.02.

14. Yushkevich PA, Piven J, Hazlett HC, et al. User-guided 3D active contour segmentation of anatomical structures: Significantly improved efficiency and reliability. *Neuroimage.* 2006;31(3):1116-1128. doi:10.1016/j.neuroimage.2006.01.015.

15. Mohamed OA, Masood SH, Bhowmik JL. Optimization of fused deposition modeling process parameters: a review of current research and future prospects. *Adv Manuf.* 2015;3(1):42-53. doi:10.1007/s40436-014-0097-7.

16. Mottini M, Seyed Jafari SM, Shafighi M, Schaller B. New approach for virtual surgical planning and mandibular reconstruction using a fibula free flap. *Oral Oncol.* 2016;59:e6-e9. doi:10.1016/j.oraloncology.2016.06.001.

17. Herrero Antón de Vez H, Herrero Jover J, Silva-Vergara C. Personalized 3D printed surgical tool for guiding the chisel during hump reduction in rhinoplasty. *Plast Reconstr Surg Glob Open.* 2018;6(2):e1668. doi:10.1097/GOX.0000000000001668.

18. Werz SM, Zeichner SJ, Berg B-I, Zeilhofer H-F, Thieringer F. 3D printed surgical simulation models as educational tool by maxillofacial surgeons. *Eur J Dent Educ.* 2018;22(3):e500-e505. doi:10.1111/eje.12332.

19. Amodeo CA. The central role of the nose in the face and the psyche: review of the nose and the psyche. *Aesth Plast Surg.* 2007;31(4):406-410. doi:10.1007/s00266-006-0241-2.

20. Federico G, Ferrante D, Marcatto F, Brandimonte MA. How the fear of COVID-19 changed the way we look at human faces. *PeerJ.* 2021;9:e11380. doi:10.7717/peerj.11380.

21. Toriumi DM. Preservation rhinoplasty. *Plast Recons Surg.* 2021;147(5):1256-1258. doi:10.1097/PRS.0000000000007911

22. Zammit D, Safran T, Ponnudurai N, et al. Step-specific simulation: the utility of 3D printing for the fabrication of a low-cost, learning needs-based rhinoplasty simulator. *Aesthetic Surg J.* 2020;40(6):NP340-NP345. doi:10.1093/asj/sjaa048.

23. Ho M, Goldfarb J, Moayer R, et al. Design and printing of a low-cost 3D-printed nasal osteotomy training model: development and feasibility study. *JMIR Med Educ.* 2020;6(2):e19792. doi:10.2196/19792.

24. Gupta N, Fitzgerald CM, Ahmed MT, Tohidi S, Winkler M. Feasibility of a 3D printed nasal model for resident teaching in rhinoplasty. *J Plast Reconstr Aesthetic Surg.* 2021:74(10):2776-2820. doi:10.1016/j.bjps.2021.05.071.